Journal of Functional Foods 73 (2020) 104154

Contents lists available at ScienceDirect

Journal of Functional Foods

journal homepage: www.elsevier.com/locate/jff

# Plant-derived peptides rubiscolin-6, soymorphin-6 and their *c*-terminal amide derivatives: Pharmacokinetic properties and biological activity

Azzurra Stefanucci[a,*], Marilisa Pia Dimmito[a], Giancarlo Tenore[b], Stefano Pieretti[c], Paola Minosi[c], Gokhan Zengin[d], Chiara Sturaro[e], Girolamo Calò[e], Ettore Novellino[b], Angelo Cichelli[f], Adriano Mollica[a]

[a] Dipartimento di Farmacia, Università di Chieti-Pescara "G. d'Annunzio", Via dei Vestini 31, 66100 Chieti, Italy
[b] Department of Pharmacy, University of Naples "Federico II", Via D. Montesano 49, 80131 Naples, Italy
[c] Istituto Superiore di Sanità, Centro Nazionale Ricerca e Valutazione Preclinica e Clinica dei Farmaci, Viale Regina Elena 299, 00161 Rome, Italy
[d] Department of Biology, Science Faculty, Selcuk University, Konya, Turkey
[e] Department of Medical Sciences, Section of Pharmacology, University of Ferrara, Italy
[f] Department of Medical, Oral and Biotechnological Sciences, "G. d'Annunzio" University Chieti-Pescara, Via dei Vestini 31, 66100 Chieti, Italy

ARTICLE INFO

*Keywords:*
Opioid peptides
Rubiscolin-6
Soymorphin-6
Antinociception
Antioxidant activity

ABSTRACT

The aim of this work is to investigate the pharmacokinetic properties, antinociceptive and antioxidant activities of rubiscolin-6, soymorphin-6 and their *C*-terminal amides; The four peptides were synthesized following Fmoc-SPPS strategy to give the final peptides in excellent overall yields and purity following analytical RP-HPLC analysis. None of them shows antioxidant activity and α-tyrosinase inhibition *in vitro*. All compounds are able to activate G-protein coupled receptor at the δ-opioid receptor (DOR) at 100 μM concentration however, rubiscolin-6-amide exhibits significative antinociceptive effect after i.c.v. administration in the tail flick test (TF) and s.c. administration in the formalin test (FT). Rubiscolin-6 shows the best *in vitro* intestinal bioavailability in CaCo2 cell monolayer and stability to the brush border exopeptidases in the apical compartment. *In silico* experiments show the interaction of rubiscolin-6 and rubiscolin-6 amide at the binding cavity of DOR compared with the crystallographic ligand TIPP-$NH_2$.

## 1. Introduction

Exogenous peptides endowed with opioid activity deriving from natural proteins, acting on plants and animals are called exorphins (Zioudrou, Streaty, & Klee, 1979). Some peptides derived from plant proteins might show beneficial effect for plant suppressing escape reaction of insects (Yang et al., 2001; Zioudrou et al., 1979). In general, such bioactive peptides may exert several pharmacological activity as receptor's ligands, enzymes inhibitors, peptides modulating transport, anti-microbial peptides and antioxidant and radical scavenger. The affinity of those peptides for opioid receptors are much smaller than the endogenous ones, however some of them exhibit central and peripheral effects after oral administration (Kaneko et al., 2012; Yoshikawa, 2015).

Accordingly, opioid peptides derived from food through protein digestion, fermentation, or food production processes could produce several benefits against some health problems, such as obesity, cardiovascular diseases, type II-diabetes and immune disorders (Stefanucci et al., 2018). Among them, soymorphins and rubiscolins recently received a great attention from researchers due to their potential applications in the development of functional foods and as lead compounds for the design of novel chemical entities.

Soymorphin (SM peptide sequence: Tyr-Pro-Phe-Val-Val-Asn-Ala) is an opioid eptapeptide derived from the enzymatic digestion of soy proteins which are consumed in cereals. Specifically, SM belongs to the enzymatic digestion of soybean β-conglycinin β-subunit by DPP-IV. The

*Abbreviations:* DOR, δ-opioid receptor; MOR, μ-opioid receptor; FT, formalin test; TF, tail flick test; BBB, blood brain barrier; s.c., subcutaneous; i.c.v., intracerebroventricular; SM, soymorphin; BCM, β-casomorphin; GPI, guinea pig ileum; MVD, mouse vas deferens; EM-1, endomorphin-1; EM-2, endomorphin-2; STZ, streptozocine; SPPS, solid phase peptide synthesis; TMS, trimethylsilane; TBTU, 2-(1H-Benzotriazole-1-yl)-1,1,3,3-tetramethylaminium tetrafluoroborate; HOBt, hydroxybenzotriazole; DIPEA, N-Ethyldiisopropylamine; DMF, dimethylformamide; TIPS, triisopropylsilane; ACN, acetonitrile; TFA, trifluoroacetic acid; ADME, absorption, distribution, metabolism, excretion

* Corresponding author.
*E-mail address:* a.stefanucci@unich.it (A. Stefanucci).

https://doi.org/10.1016/j.jff.2020.104154
Received 30 April 2020; Received in revised form 28 July 2020; Accepted 7 August 2020

shorter sequence YPFVV found in the *C*-terminal region of β-conglycin β subunit is the homologue of human β-casomorphin-5 (YPFVE) named soymorphin-5 (Yoshikawa, 2015).

β-conglycin β subunit releases soymorphin-5 by pancreatic elastase and leucine aminopeptidase, while soymorphin-6 (YPFVVN) is obtained by the action of pepsin and pancreatic elastase. Soymorphin-6 (SM-6) possesses anxiolytic (at a dose of 100 mg/kg in elevated-plus maze experiment in mice) and anorexygenic effects after oral administration in animal models (at a dose of 36 mg/kg in 18-h fasted mice, four hours after administration), together with a selective MOR opioid activity in GPI and MVD assays which is two fold more potent than β-casomorphin (BCM) (Arısoy & Üstün-Aytekin, 2018; Kaneko, Iwasaki, Yoshikawa, & Ohinata, 2010; Ohinata, Agui, & Yoshikawa, 2007; Yoshikawa, 2015).

This hexapeptide shares the sequence YPFV with the human β-casomorphin-4, an opioid peptide with morphine-like activity. Endomorphin-1, -2 (EM-1 and EM-2) and hemorphin (YPWT) derived from hemoglobin, containing the sequence Tyr-Pro-aromatic amino acid are also μ-selective opioid peptides of natural origin (Dvoracsko, Stefanucci, Novellino, & Mollica, 2017; Torino et al., 2010). In contrast opioid peptides derived from plants such as gluten exorphin and rubiscolin containing the sequence Tyr-Pro-non aromatic amino acids, are selective for the δ-opioid receptors (Ohinata et al., 2007).

Rubiscolin-6 (amino acid sequence: YPLDLF) is an opioid peptide derived from the plant enzyme Rubisco, which is responsible for $CO_2$ fixation in green leaves, but it is also a food source in the biosphere (Kaneko et al., 2012; Yoshikawa, 2015).

Rubiscolin-6 exhibits memory-enhancing, anxiolytic and orexygenic activities in animal models (Hirata et al., 2007). Rubiscolin-6 is also able to bind both δ and μ-opioid receptors with a good to moderate affinity respectively (IC50δ 0.93 μM *vs*. $IC50_{\mu} > 2000$ μM), showing a strong selectivity for DOR. This activity is related to the ability of Rubiscolin-6 to stimulate glucose uptake in L6 and C2C12 cells, in enhancement of GLUT4 expression through the AMPK pathway, and improvement of glucose homeostasis in STZ-induced diabetic rats (Hirata et al., 2007).

Rubiscolin-6 produces antinociceptive effect after i.c.v. administration at a minimum dose of 3 nmol/mouse and 1 nmol/mouse using *in vivo* tail pinch method. It exhibits antinociceptive effect *in vivo* after oral administration at 300 mg/kg, mediated by δ-opioid receptors; in fact, the selective δ-opioid receptor antagonist naltrindole blocks antinociception induced by Rubiscolin-6 (Miyazaki et al., 2014). Due to its interesting spectra of biological activities on diverse organic systems, rubiscolin-6 is considered as *lead compound* for building a rational structure-activity relationship study (Yang, Sonoda, Chen, & Yoshikawa, 2003).

In order to identify the amino acid residues essential for its opioid activity, Rubiscolin-6 derivatives were synthesized and among them δ-opioid activities of [$Ile^3$]-rubiscolin-6 and [$Met^3$]-rubiscolin-6 were four fold higher than that of rubiscolin (Yang et al., 2001).

The most potent analogue discovered so far was [$Met^3$,$Val^6$]-rubiscolin-6 with 20 fold higher potency than the reference exogenous compound (Ohinata et al., 2007; Yoshikawa, 2015).

Considering the panel of peripheral and central effects exerted by these natural bioactive peptides (Hirata et al., 2007; Kaneko et al., 2012; Miyazaki et al., 2014; Perlikowska & Janecka, 2018), we planned to prepare Rubiscolin-6 and Soymorphin-6 as *lead compounds* and their *C*-terminal amide analogues following solid phase peptide synthesis (SPPS). The antioxidant, α-tyrosinase inhibition activities and G protein stimulation at DOR and MOR with calcium mobilization assay have been evaluated *in vitro, in vivo* antinociceptive effects have been also studied through tail flick and formalin tests after i.c.v. and s.c. administration, respectively. Intestinal bioavailability in CaCo2 cell monolayer was also investigated in order to define their possible oral bioavailability and to assess stability to exopeptidases in the brush border. Furthermore, *in silico* molecular modeling study was performed with the aim to reveal the binding mode at the DOR of rubiscolin-6 and its *C*-terminal amide.

The aim of this project is to investigate the biological and pharmacokinetic properties of opioid plant-derived peptides soymorphin-6, rubiscolin-6 and their novel *C*-terminal amides derivatives.

## 2. Materials and methods

### 2.1. Chemicals and reagents

Chemicals and reagents were purchased by VWR (MI, Italy) and Merck (MI, Italy), amino acids from GLS Shanghai (China). Final crude peptides were purified on C18 prep RP-HPLC at 216, 235, 254, and 275 nm (Waters C18 4.6 mm × 150 mm); flow rate of 7 mL/min; gradient eluent of $H_2O$/ACN-0.1% TFA, from 5% ACN to 90% ACN in 32 min. Pure peptides were identified by $^1$H NMR at 25 °C on a 300 MHz Varian Oxford spectrometer, DMSO-$d_6$ as solvent and chemical shifts in parts per million (δ) downfield from the internal standard TMS. LCQ Finnigan-Mat mass spectrometer (San Jose, CA) equipped with ESI-spray source and ion trap analyzer was used at capillary temperature of 200 °C, spray voltage at 4.00 kV and nitrogen and helium as sheath and auxiliary gas respectively.

### 2.2. Peptides and chemical characterization

Soymorphin-6, Rubiscolin-6 and their *C*-terminal amide analogues were prepared following the well-established Fmoc-solid phase peptide synthesis (Fmoc-SPPS) and were purified by reverse-phase high-performance liquid chromatography (RP-HPLC) (Poli et al., 2019; Stefanucci et al., 2019). The purity of four peptides was checked by analytical RP-HPLC at 236, 268 and 214 nm (C18-bonded 4.6 mm × 150 mm), flow rate of 1 mL/min, using a gradient of $H_2O$/ACN-0.1% TFA from 5% to 95% ACN in 26 min, and was found to be ≥95%. Peptide structures were identified by $^1$H NMR spectrometry and LRMS (see SI).

### 2.3. In vitro antioxidant activity

For antioxidant capacity, different test systems, including radical quenching (DPPH and ABTS), reducing power (CUPRAC and FRAP), were used. The methods details were described in our earlier paper (Grochowski et al., 2017; Zengin et al., 2019). Trolox equivalents were selected as standards and compounds abilities were expressed as equivalents of trolox (mg TE/g). The significance of differences ($p < 0.05$) among the peptides was calculated using the parametric One-way ANOVA test together with Tukey's test (GraphPad Prism 6.0).

### 2.4. α-tyrosinase inhibition assay

For the tyrosinase inhibition assay, we used L-DOPA (as substrate) and mushroom tyrosinase enzyme (E.C. 1.14.18.1) (Luisi, Stefanucci, Zengin, Dimmito, & Mollica, 2018).

Kojic acid was used as a standard inhibitor and the results were expressed as kojic acid equivalents (mg KAE/g) the significance of differences ($p < 0.05$) among the peptides was calculated using the parametric One-way ANOVA test together with Tukey's test (GraphPad Prism 6.0).

### 2.5. In vitro calcium mobilization assay

#### 2.5.1. Drugs and reagents

Brilliant black, bovine serum albumin (BSA), 4-(2- hydroxyethyl)-1-piperazineethanesulfonic acid (HEPES), and probenecid were from Sigma Aldrich (St. Louis, MO, USA). Pluronic acid and Fluo-4 AM were from Thermo Fisher Scientific (Waltham, US). All cells culture media and supplements were from Euroclone (Milano, Italy). Rubiscolin-6, rubiscolin-6 *C*-amide, soymorphin-6, soymorphin-6 *C*-amide,

endomorphin-1 (EM-1) were dissolved in dimethyl sulfoxide (DMSO) at the concentration of 10 mM. The stock solutions were kept at −20 °C until use.

#### 2.5.2. Cells

CHO cells lines permanently co-expressing μ-receptors with the *C*-terminally modified $G\alpha_{qi5}$ and δ-receptors with the *C*-terminally modified $G\alpha_{qG66Di5}$, were used. Details regarding the generation of these cells have been previously described (Camarda et al., 2009; Lambert & Rainbow, 2013).

Cells were cultured in culture medium consisting of Dulbecco's modified Eagle's medium (DMEM) / HAMS F12 (1:1) supplemented with 10% fetal bovine serum (FBS), penicillin (100 IU/mL), streptomycin (100 mg/mL), geneticin (G418; 200 μg/mL) and hygromycin B (100 μg/mL). Cell cultures were kept at 37 °C in 5% $CO_2$ / humidified air. When confluence was reached (3–4 days), cells were sub-cultured as required using trypsin / EDTA and used for experimentation. Cells were seeded at a density of 50,000 cells / well into 96-well black, clear-bottom plates. After 24 h incubation the cells were loaded with Hank's Balanced Salt Solution (HBSS) supplemented with 2.5 mM probenecid, 3 μM of the calcium sensitive fluorescent dye Fluo-4 AM, 0.01% pluronic acid and 20 mM HEPES (pH 7.4) for 30 min at 37 °C. Afterwards the loading solution was aspirated and a washing step with 100 μL/well of HBSS, HEPES (20 mM, pH 7.4), 2.5 mM probenecid and 500 μM Brilliant Black was carried out. Subsequently 100 μL/well of the same buffer was added. After placing cell culture and compound plates into the FlexStation II (Molecular Devices, Sunnyvale, CA, USA), changes in fluorescence of the cell-loaded calcium sensitive dye Fluor-4 AM were measured. On-line additions were carried out in a volume of 50 μL/well.

#### 2.5.3. Data analysis and terminology

All data were analyzed using Graph Pad Prism 6.0 (La Jolla, CA, USA). Data are expressed as mean ± sem of *n* experiments performed in duplicate. In calcium mobilization studies, agonist effects were expressed as maximum change in percent over the baseline fluorescence. Baseline fluorescence was measured in wells treated with vehicle. Agonist potency was expressed as $pEC_{50}$, which is the negative logarithm to base 10 of the agonist molar concentration that produces 50% of the maximal possible effect of that agonist. Concentration response curve to agonists were fitted with the four-parameter logistic non-linear regression model:

$$\text{Effect} = \text{Baseline} + \frac{E_{\max} - \text{Baseline}}{\left(1 + 10^{LogEC_{50}Log_{[compound]}Hillslope}\right)}$$

### 2.6. In vivo antinociceptive assays

#### 2.6.1. Animals

CD-1 male mice (Charles River, Italy) weighing 25–30 g were used in all experiments. Before the experimental sessions, the mice were maintained in colony, housed in cages (7 mice per cage) under standard light/dark cycle (from 7:00 AM to 7:00 PM), temperature (21 ± 1 °C) and relative humidity (60 ± 10%) for at least 1 week. Food and water were available *ad libitum*. The research protocol was approved by the Service for Biotechnology and Animal Welfare of the Istituto Superiore di Sanità and authorized by the Italian Ministry of Health, according to Legislative Decree 26/14, which implemented the European Directive 2010/63/UE on the protection of laboratory animals in Italy. Animal welfare was routinely checked by veterinarians from the Service for Biotechnology and Animal Welfare.

#### 2.6.2. Tail flick test

The tail flick test was used to determinate antinociceptive response induced by a thermal stimulus and was performed as described earlier (Dimmito et al., 2019). Tail flick apparatus (Ugo Basile, Varese, Italy) consists of an infrared radiant light source (100 W, 15 V bulb) targeted on a photocell utilizing an aluminum parabolic mirror. During the trials, the mice were gently hand restrained with a glove. Radiant heat was targeted 5–6 cm from the tip of the tail, and the latency (s) of the tail withdrawal recorded. The measurement was disconnected if the latency crossed the cutoff time. A cutoff time of 15 s was imposed, and data were expressed as time course of the percentage of maximum effect (% MPE) = (post drug latency/baseline latency)/(cutoff time baseline latency) × 100. In all experiments, the baseline was calculated as the mean of three readings recorded before testing at intervals of 10 min, and the time course of latency was determined 10–120 min after compound treatment. Compounds were freshly diluted in saline containing 0.1% v/v DMSO, and were injected at 10 μg/10 μL for intracerebroventricular (i.c.v.) administrations, as previously reported (Mollica et al., 2013; Piekielna-Ciesielska et al., 2018).

#### 2.6.3. Formalin test

The method utilized was comparable to the one previously described (Mollica et al., 2011).

Subcutaneous injection of 20 μL of a 1% solution of formalin in saline into the dorsal surface of the mouse hind paw evoked nociceptive behavioural responses, such as licking, biting the injected paw, or both, which are considered indices of nociception. The nociceptive response showed a biphasic trend: an early phase, occurring from 0 to 10 min after formalin injection, produced by the direct stimulation of peripheral nociceptors, and a late prolonged phase, occurring from 15 to 40 min, which reflected the response to inflammatory pain. During the test, the mouse was placed in a Plexiglas observation cage (30 × 14 × 12 cm), 1 h before the formalin administration and allowed to acclimatize to the testing environment. Compounds were solubilized in saline (0.9% NaCl in distilled water) and DMSO in the ratio DMSO:saline 1:3 (v/v) and were administered subcutaneously in the dorsal surface of the right hind paw of the mouse using a microsyringe with a 27-gauge needle 15 min before formalin injection at the dose of 100 μg/20 μL. Then, the total time the animal spent licking or biting its paw in the early and late phase was recorded.

#### 2.6.4. Statistical analysis

Statistically significant differences between groups in the tail flick test and formalin test were measured with a two-way analysis of variance (2-ANOVA) followed by Tukey's or Sidak's post-hoc comparisons. GraphPad Prism 6.0 software (San Diego, CA, USA) was used to analyze the data. Data were considered statistically significant when a value of $p < 0.05$ was performed.

### 2.7. In vitro gastrointestinal digestion

#### 2.7.1. Reagents and standards

All chemicals and reagents used were either analytical-reagent or HPLC grade. The water was treated in a Milli-Q water purification system (Millipore, Bedford, MA, USA) before use. Chemicals and reagents to simulate the GI digestion were: potassium chloride (KCl), potassium thiocyanate (KSCN), monosodium phosphate ($NaH_2PO_4$), sodium sulphate ($Na_2SO_4$), sodium chloride (NaCl), sodium bicarbonate ($NaHCO_3$), urea, α-amylase, hydrochloric acid (HCl), pepsin, pancreatin, bile salts (Sigma Chemical Co., St. Louis, MO, USA). All organic solvents were purchased from Carlo Erba, (Milano, Italy). 2′,7′-dichlorofluorescin diacetate (DCFH-DA, Sigma Chemical Co.) was dissolved in dimethylsulfoxide (DMSO) to obtain 100 mM stock solution (aliquoted and stored at −20 °C). Work solutions of DCFH-DA were produced by diluting aliquots in 1% phosphate buffer saline (PBS, 10 mM, pH 7.4) at different concentrations. The assay was performed according to the procedure described by Raiola, Meca, Mañes, and Ritieni (2012), with slight modification (Raiola et al., 2012).

GI digestion was distinguished into salivary, gastric and duodenal

digestive steps. For the salivary digestion, an aliquot of each peptide (1.0 mg) was mixed with 6 mL of artificial saliva composed of: KCl (89.6 g/L), KSCN (20 g/L), $NaH_2PO_4$ (88.8 g/L), $Na_2SO_4$ (57.0 g/L), NaCl (175.3 g/L), $NaHCO_3$ (84.7 g/L), urea (25.0 g/L) and 290 mg of α-amylase. The pH of the solution was adjusted to 6.8 with 0.1 M HCl. The mixture was introduced in a plastic bag containing 10 mL of water and homogenized in a Stomacher 80 Microbiomaster (Seward, Worthing, UK) for 3 min. Immediately, 0.5 g of pepsin (14,800 U) dissolved in HCl 0.1 N was added, the pH was adjusted to 2.0 with 6 M HCl, and then incubated at 37 °C in a Polymax 1040 orbital shaker (250 rpm) (Heidolph, Schwabach, Germany) for 2 h. After the gastric digestion, the pancreatic digestion was simulated as follows: the pH was increased to 6.5 with 0.5 M $NaHCO_3$ and then 5 mL of a mixture pancreatin (8.0 mg/mL) and bile salts (50.0 mg/mL) (1:1; v/v), dissolved in 20 mL of water, were added and incubated at 37 °C in an orbital shaker (250 rpm) for 2 h. Intestinal digested sample was freeze-dried and stored at −80 °C until further analysis.

#### 2.7.2. HPLC-DADA analyses

Intestinal digested samples were filtered through a Phenex-PVDF 17 mm Syringe Filter 0.45 µm (Phenomenex, Torrance, CA, USA) and analysed by RP-HPLC. Analyses were run on a Finnigan HPLC system (Thermo Electron Corporation, San Jose, CA, USA) provided with photodiode array detector (DAD). The column selected was a Aeris PEPTIDE 3.6 µm XB-C18 New Column 250 × 4.6 mm (Phenomenex). Elution conditions consisted in 2% acetic acid (solvent A) and 2% acetic acid in methanol (solvent B) gradient at a flow rate of 1.0 mL/min. The gradient conditions were: 0–20 min, 0–100% B; 20–23 min, 100% B; 23–27 min, 0% B, followed by 5 min of maintenance. Chromatograms were recorded at 280 nm.

#### 2.7.3. In vitro intestinal stability and transepithelial transport studies

The assay was performed as previously described by Tenore, Campiglia, Giannetti, and Novellino (2015).

### 2.8. Molecular modeling study

Molecular modeling study was performed on rubiscolin-6 and rubiscolin-6 *C*-amide using Maestro 2017, following the well-established procedure reported by Stefanucci et al. (2020).

## 3. Results

### 3.1. Antioxidant and tyrosinase inhibition activities of synthetic peptides

The antioxidant abilities of the synthetic peptides were investigated by DPPH, ABTS, FRAP and CUPRAC methods. The results are in Table 1. The highest DPPH radical scavenging ability was found for rubiscolin-6 *C*-amide, followed by soymorphin, rubiscolin-6 and soymorphin-6 *C*-amide, while the best ABTS radical ability was recorded by soymophin-6 *C*-amide. In FRAP assay, rubiscolin-6 *C*-amide showed the highest potential with the value of 5.79 mg TE/g. However, there was no significant differences in FRAP values among rubiscolin-6, rubiscolin-6 *C*-amide and soymorphin-6 *C*-amide. As shown in Table 1, rubiscolin-6 exhibited the best tyrosinase inhibition ability with a value of 24.51 mg KAE/g, followed by soymorphin-6 *C*-amide and rubiscolin-6 *C*-amide. Soymorphin-6 is not active on tyrosinase.

### 3.2. Calcium mobilization assay

In these experiments we evaluated the capability of the compounds to activate the µ- and δ-human recombinant receptors permanently transfected in CHO cells. In such cells the expression of a chimeric G protein that forces the opioid receptors to couple with the calcium pathway allows measuring receptor activation with an automated calcium mobilization assay. Dermorphin and DPDPE were used as standard ligands for µ- and δ-receptors, respectively. In $CHO_\mu$ cells the standard agonist dermorphin evoked a robust concentration-dependent stimulation of calcium release displaying high potency ($pEC_{50}$ of 8.06) and maximal effects (254 ± 18% over the basal values). EM-1 mimicked the stimulatory effect of dermorphin showing similar maximal effects but 3-fold lower potency ($pEC_{50}$ of 7.45). Rubiscolin-6 *C*-amide, Soymorphin-6 and Soymorphin-6 *C*-amide stimulated calcium mobilization only at micromolar concentrations eliciting incomplete concentration response curves, while Rubiscolin-6 was completely inactive. The concentration response curves obtained with these ligands in $CHO_\mu$ cells are displayed in Fig. S1 (see SI) and their pharmacological parameters summarized in Table 2. In $CHO_\delta$ cells the standard agonist DPDPE evoked a robust concentration-dependent stimulation of calcium release displaying high potency ($pEC_{50}$ of 7.51) and maximal effects (223 ± 17% over the basal values). All the other compounds showed an incomplete concentration response curve, being active only at micromolar concentrations. The concentration response curves obtained with these ligands in $CHO_\delta$ cells are displayed in Fig. S2 (see SI) and their pharmacological parameters summarized in Table 2.

### 3.3. Antinociceptive effects of Rubiscolin-6 C-amide and Soymorphin-6 C-amide

The antinociceptive effect of Rubiscolin-6 and Rubiscolin-6 *C*-amide are reported in Fig. 1. In the tail flick test, Rubiscolin-6 induced a significant antinociceptive effect 15 min after administration, followed by a rapid decrease, which becomes similar to that observed in vehicle-treated animals from 60 to 120 min after administration. On the contrary Rubiscolin-6 *C*-amide induced a robust and significant antinociceptive effect, which is observed 15 min later and which light decreased up to 120 min after administration (Fig. 1). In the formalin test, Rubiscolin-6 was not able to change the nociceptive effect of formalin, both in the early and in the late phase of the test. As previously observed in the tail flick test, Rubiscolin-6 *C*-amide provoked an antinociceptive effect since it reduced formalin-induced nociception in both test phases (Fig. 1). In Fig. 2 are reported the effects of Soymorphin-6 and Soymorphin-6 *C*-amide in the tail flick and formalin tests. Soymorphin-6 and Soymorphin-6 *C*-amide induced similar effects in these tests. Both peptides exerted significant antinociceptive effect 15 and 30 min after the administration, followed by a gradual and similar decrease in the antinociception. In the formalin test, both peptides did not change the nociceptive effects of formalin in the early phase of the test. In the late phase of the formalin test, Soymorphin-6 induced a light increase and Soymorphin-6 *C*-amide a light decrease of the nociceptive

**Table 1**
Antioxidant properties and tyrosinase inhibitory effects of the tested peptides.*

| Peptides | DPPH (mg TE/g) | ABTS (mg TE/g) | CUPRAC (mg TE/g) | FRAP (mg TE/g) | Tyrosinase inhibition (mg KAE/g) |
|---|---|---|---|---|---|
| Rubiscolin-6 | 2.41 ± 0.33$^a$ | 8.86 ± 0.38$^b$ | 10.09 ± 0.02$^a$ | 5.75 ± 0.04$^a$ | 24.51 ± 1.99$^a$ |
| Soymorphin-6 | 2.65 ± 0.70$^a$ | 3.09 ± 0.47$^c$ | 9.10 ± 0.08$^b$ | 5.64 ± 0.04$^b$ | na |
| Rubiscolin-6 *C*-amide | 2.72 ± 0.51$^a$ | 0.77 ± 0.01$^d$ | 9.55 ± 0.05$^c$ | 5.79 ± 0.03$^a$ | 2.81 ± 0.34$^c$ |
| Soymorphin-6 *C*-amide | 1.38 ± 0.21$^b$ | 11.00 ± 1.96$^a$ | 9.35 ± 0.13$^c$ | 5.72 ± 0.08$^a$ | 9.19 ± 1.43$^b$ |

* Values are reported as mean ± S.D of three parallel experiments. TE: Trolox equivalents; KAE: Kojic acid equivalents; na: not active. a-d: Different letters indicate significant differences in the peptides ($p < 0.05$).

**Table 2**
Potencies ($pEC_{50}$) and maximal effects of standard and novel ligands at μ and δ -opioid receptors.

| | $CHO_{\mu}$ | | $CHO_{\delta}$ | |
|---|---|---|---|---|
| Compounds | $pEC_{50}$ ($CL_{95\%}$) | $E_{max}$ ± sem % | $pEC_{50}$ ($CL_{95\%}$) | $E_{max}$ ± sem % |
| Dermorphin | 8.06 (7.65–8.46) | 254 ± 18% | 6.43 (5.95–6.91)[a] | 78 ± 3%[a] |
| DPDPE | Inactive[a] | | 7.51 (7.31–7.70) | 223 ± 17% |
| EM-1 | 7.45 (7.08–7.82) | 263 ± 30% | Crc incomplete, at 100 μM 89 ± 15% | |
| Rubiscolin-6 | Inactive | | Crc incomplete, at 100 μM 87 ± 19% | |
| Rubiscolin-6 *C*-amide | Crc incomplete, at 100 μM 131 ± 29% | | Crc incomplete, at 100 μM 112 ± 29% | |
| Soymorphin-6 | Crc incomplete, at 100 μM 110 ± 13% | | Crc incomplete, at 100 μM 46 ± 14% | |
| Soymorphin-6 *C*-amide | Crc incomplete, at 100 μM 81 ± 4% | | Crc incomplete, at 100 μM 79 ± 14% | |

Data are mean of at least 5 separate experiments made in duplicate.
[a] Values taken from (Camarda et al., 2009).

effect provoked by formalin, but both effects were not statistically significant in comparison with vehicle-treated animals.

### 3.4. In vitro intestinal bioaccessibility

Results shown in Table 3 clearly indicate a quite high susceptibility of the peptides to the *in vitro* gastrointestinal environment. Specifically, their amide derivatives are the least resistant to the chemical and enzymatic conditions of the simulated digestive protocol. The intestinal stability and bioavailability of peptides were evaluated by using single layers of CaCo2 cells as a model of absorption in the small intestine. HPLC analysis highlighted very moderate hydrolysis of Rubiscolin-6 and Soymorphin-6 (less than 10% and 15%, respectively) in the apical solution by the brush border exopeptidases after 120 min incubation and regardless of the peptide concentration (Fig. S3, see SI). Differently, their respective amide derivatives revealed an important susceptibility to enzymatic degradation, showing average hydrolysis rates of 74% and 65% for Rubiscolin-6 *C*-amide and Soymorphin-6 *C*-amide, respectively. HPLC analyses of basolateral solution revealed that all peptides were absorbed intact through CaCo2 monolayer, with a concentration-dependent transport following a saturable pattern described by a linear curve (Fig. 3). Interestingly, the actual amount of Rubiscolin-6 and Soymorphin-6 transepithelially transported was about 10%, thus higher than what generally reported for different size (3–17 aminoacid units) and polarity peptides transported from CaCo2 monolayer apical to basolateral side (Okumu, Pauletti, Vander Velde, Siahaan, & Borchardt, 1997; Regazzo et al., 2010; Satake et al., 2002).

### 3.5. Docking study

*In silico* molecular modeling approach was applied to investigate the relationship between the bioactivity found *in vitro* and *in vivo* by rubiscolin-6 and its *C*-terminal amide and their interactions at the δ-opioid receptor (DOR). The docking of the two peptides was performed on the crystal structure of the DOR (4RWD) downloaded from the PDB database and the so obtained poses have been compared with crystallographic ligands. The receptor was prepared for the docking experiments as previously reported (Stefanucci et al., 2019, 2020) with the PrepWizard module embedded in Maestro 2017 (Schrödinger Release, 2016). The missing side chains were added, and all the co-crystallized molecules were removed except for the opioid ligand TIPP-$NH_2$ and the water molecules 1303 and 101 which are fundamental for the correct activation of the receptor (Kaserer, Lantero, Schmidhammer, Spetea, & Schuster, 2016). These water molecules are necessary for a correct and predictable docking procedure (Kaserer et al., 2016; Stefanucci et al., 2019, 2020). Thus in this model is present a water network connecting the ligand to a key residue of Histidine 278.

After the preparation steps, the docking was performed by using the software Gold 6.0 with a docking procedure previously validated by our group (Stefanucci et al., 2019, 2020). The fitness functions GOLDSCORE was employed for these experiments basing on our previous studies (Stefanucci et al., 2019, 2020). The two water molecules were set to "toggle and spin", in order to allow the program to automatically decide whether the water molecules should be included during the docking and to optimize their orientation. An area of 10 Å around the co-crystallized ligand was defined as the binding site.

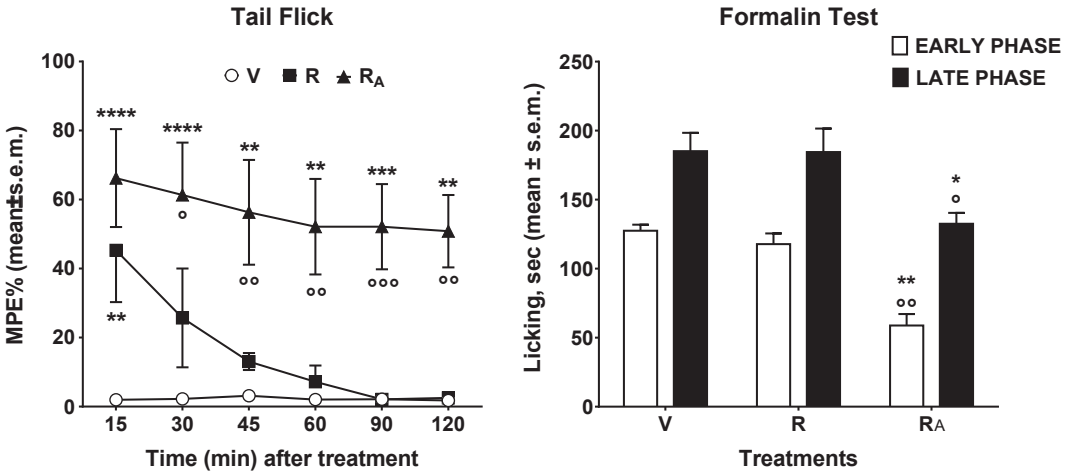


**Fig. 1.** Effects induced by Rubiscolin-6 (R) and Rubiscolin-6 *C*-amide ($R_A$) in the tail flick test (left panel) and in the formalin test (right panel). In the tail flick test, compounds were administered i.c.v. at the dose of 10 μg/10 μL; in the formalin test, compounds were administered s.c., in the dorsal surface of the mouse hind paw, at the dose of 100 μg/20 μL, 15 min before formalin. V is for vehicle-treated animals. ** is for $P < 0.01$, *** is for $P < 0.001$, **** is for $P < 0.0001$ *vs* V; ° is for $P < 0.05$, °° is for $P < 0.01$, °°° is for $P < 0.001$ *vs* R. N = 7.

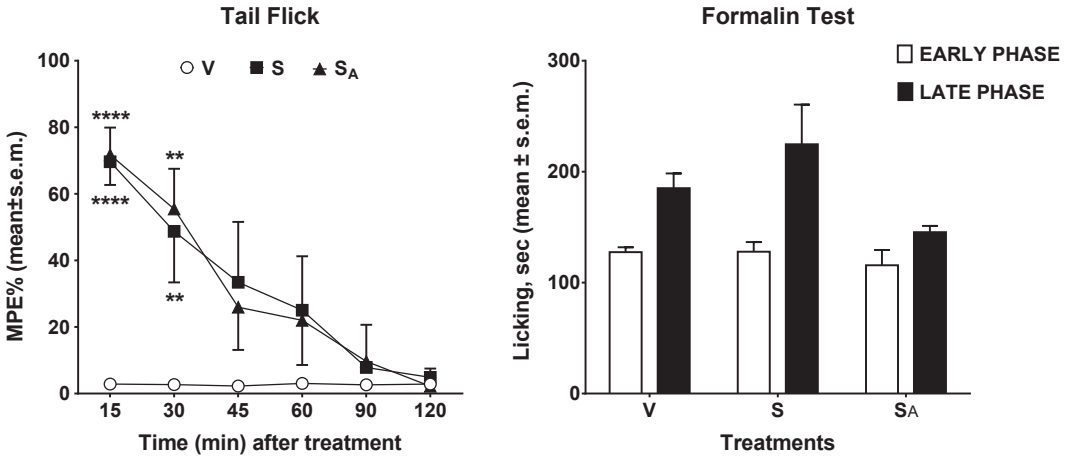


**Fig. 2.** Effects induced by Soymorphin-6 (S), Soymorphin-6 *C*-amide (SA) in the tail flick test (left panel) and in the formalin test (right panel). In the tail flick test, compounds were administered i.c.v. at the dose of 10 μg/10 μL; in the formalin test, compounds were administered s.c., in the dorsal surface of the mouse hind paw, at the dose of 100 μg/20 μL, 15 min before formalin. V is for vehicle-treated animals. ** is for P < 0.01, **** is for P < 0.0001 *vs* V. N = 7.

**Table 3**
*In vitro* intestinal bioaccessibility of peptides calculated as area under curve of chromatograms from HPLC-DAD analyses of intestinal digesta.

| Peptide | % |
|---|---|
| Rubiscolin-6 | 10.2 ± 1.2 |
| Soymorphin-6 | 7.3 ± 0.8 |
| Rubiscolin-6 *C*-amide | 5.4 ± 0.4 |
| Soymorphin-6 *C*-amide | 3.2 ± 0.3 |

Values are the means ± SD ($n$ = 5; $P$ < 0.01).

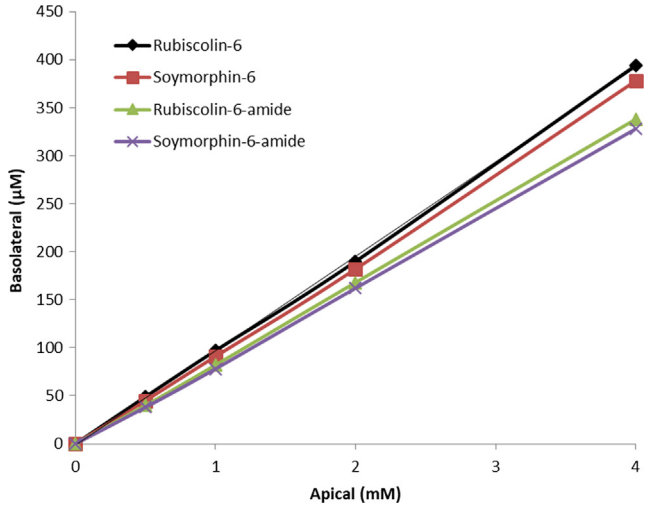


**Fig. 3.** *In vitro* intestinal bioavailability of peptides. Quantification of peptides in CaCo2 cell monolayer apical and basolateral solutions using a five-point calibration curve of pure peptides as standard analysed by HPLC.

The best poses found are reported in Fig. 4; At the DOR, both rubiscolin-6 and rubiscolin-6 *C*-amide showed a similar interaction behavior, by assuming a convergent conformation and by establishing similar interactions to the key residues Asp128, His278 and water network.

TIPP-$NH_2$ interacts with residues Asp128, His278, Trp284, Leu200 and Arg192, which are partially present in rubiscolin-6 and rubiscolin-6 *C*-amide poses.

Indeed, rubiscolin-6 is able to bind to the accessory residue Arg192, whereas this interaction is missing in its amide derivative, which preferentially bind the residue Leu200. Both of them lack to interact with Trp284, which is involved in a key interaction present in the crystallographic ligand; on the other hand they show the three main interactions to the water 101, Asp128 and His278 through the water network, which are responsible for the opioid activity found.

However, both peptides weakly bind to DOR in our calcium mobilization assay and are capable of stimulating the activation of G protein coupled to DOR at high doses (Table 2). This binding behavior falling in the micromolar range, could be explained by the lacking of those additional interactions found for TIPP-$NH_2$ (Trp284) and by the non-simultaneous presence of the interactions to Leu200 and Arg192, which could justify the low potency of rubiscolin-6 and rubiscolin-6 *C*-amide. The interactions found for both peptides, together with those of the crystallographic ligand have been reported in Table 4.

## 4. Discussion

Exorphins from plant proteins and their synthetic derivatives could exhibit a plethora of biological activity acting as modulating agents, antioxidants and anti-microbial compounds on diverse human targets such as receptors, cell's membrane and enzymes. Thus, such peptides contain certain desirable functional properties that could make them suitable in several formulated food systems.

In the present paper, we detected antioxidant properties by using different methods (DPPH, ABTS, CUPRAC and FRAP) (Kim, Lee, Lee, & Lee, 2002; Mareček et al., 2017). Generally, the tested peptides exhibit low antioxidant abilities. Rubiscolin-6 *C*-amide shows the best DPPH scavenging ability while soymorphin-6 *C*-amide exhibits the best ABTS scavenging ability. Reducing abilities of the tested peptides were evaluated by CUPRAC and FRAP assays, which indicate low electron-donating abilities for all of them. This could be due to the presence of the hydrophobic amino acids such as proline, glycine and methionine in the peptides that can contribute to the reduction abilities because of high electron density (Nwachukwu & Aluko, 2019). Literature reports that tyrosine and phenylalanine containing oligopeptides and long sequence peptides could present tyrosinase inhibitory activity (Pillaiyar, Manickam, & Namasivayam, 2017). Tyrosinase is one key enzyme in the synthesis of melanin, which is an important pigment for protection of the eye and skin from sunlight (Schurink, van Berkel, Wichers, & Boeriu, 2007). Thus novel and safe tyrosinase inhibitors are gaining interest among scientific research topics due to their importance in the prevention of hyperpigmentation problems such as melisma and age spots (Zolghadri et al., 2019). Furthermore, recent results indicate that opioids play a key role in skin homeostasis by modulating keratinocyte differentiation, wound healing and inflammation (Bigliardi-Qi et al.,

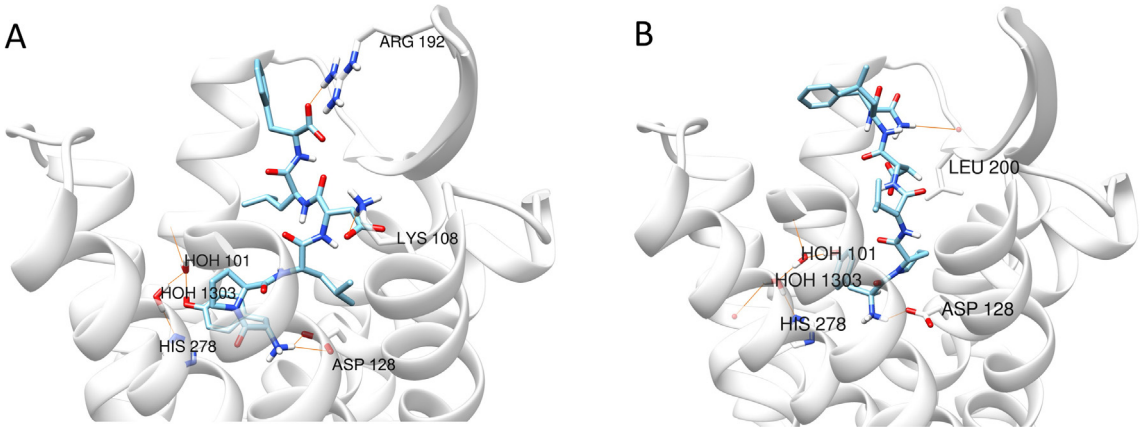


**Fig. 4.** Best ranked docking poses of Rubiscolin-6 (A) and Rubiscolin-6 *C*-amide (B) docked at the DOR (4RWD).

**Table 4**
Interactions list found in the best pose of TIPP-$NH_2$, rubiscolin-6 and rubiscolin-6*C*-amide to DOR.

| DOR interactions | | | | | |
|---|---|---|---|---|---|
| Compounds | Asp128 | His278 | Trp284 | Leu200 | Arg192 |
| TIPP-$NH_2$ | H bond | H bond through water network | π-π | H bond | Cat-π |
| Rubiscolin-6 | Ionic + H bond | H bond through water network | – | – | H bond |
| Rubiscolin-6 *C*-amide | Ionic + H bond | H bond through water network | – | H bond | – |

2006; Schmelz & Paus, 2007); β-endorphin and MOR are expressed in human epidermal melanocyte (EM) cells and they are closely associated to melanosomes. Kauser and co-workers (Kauser, Schallreuter, Thody, Gummer, & Tobin, 2003) demonstrated that they up-regulate melanocyte dendricity, proliferation, pigmentation and hair growth (Furkert et al., 1997; Tobin & Kauser, 2005) via melanocortin-1 receptor (MC-1R) independent mechanism, thus the discovery of a peptide with exogenous opioid-like structure able to inhibit tyrosinase enzyme could be useful to better understand the relationship between hyperpigmentation process and opioid peptide system. All our peptides exhibit moderate tyrosinase inhibitory effect with the only exception of soymorphin-6 which is inactive; among them rubiscolin-6 shows the best value. Calcium mobilization assay data reveal that all compounds are able to stimulate the DOR and MOR at 100 μM concentration, however rubiscolin-6 is inactive at MOR according to literature data (Hirata et al., 2007).

Overall, detailed pharmacological features of rubiscolin-6, soymorphin-6, and their *C*-amide derivatives could not be investigated due to their low potency in the present calcium mobilization assay. *In vivo* experiments confirm the previously reported antinociceptive effects of rubiscolin-6 in the experimental model of acute pain in laboratory animals (Yang et al., 2001, 2003).

Rubiscolin-6 was able to increase the nociceptive threshold to thermal stimuli after supraspinal administration, but was ineffective after subcutaneous administration in an experimental paradigm of chemical-induced nociception as the formalin test. Rubiscolin-6 *C*-amide centrally administered demonstrates a strong antinociceptive effect higher than the parent compound, and it is effective after subcutaneous administration. To the best of our knowledge no data are available on the *in vivo* effects of Soymorphin-6, thus these results are novel and firstly described. After central administration in the tail flick test, both soymorphin-6 and its derivative soymorphin-6 *C*-amide induce a robust antinociceptive effect until 30 min after the administration but both peptides are not able to change the behavioral response to chemical-induced nociception in the formalin test. All peptides were absorbed intact through CaCo2 monolayer however, rubiscolin-6 *C*-amide exhibits the most interesting *in vivo* biological profile, which prompt us to further investigate its effect after oral administration.

The carrier-mediated transport systems involving the $H^+$-coupled PepT1 transporter, may be excluded since they are active and saturable symporters specific for intestinal absorption of charged di- and tripeptides (Brandsch, Knütter, & Bosse-Doenecke, 2008). The average polar properties of these peptides would also exclude a possible passive transcellular diffusion since a vescicular-mediated internalization, the main mechanism involved, would imply absorption by apical cell membrane through hydrophobic interactions (Knipp, Velde, Siahaan, & Borchardt, 1997). The low level of degradation of rubiscolin-6 and soymorphin-6 in transepithelial transfer indicates that passive transcellular diffusion could be partially involved in their transport. In fact, the amino acids ability to join hydrogen bonds with lipid phosphates of cell membranes, has been reported as a key physicochemical feature helping the translocation process via transcytosis route (Pauletti et al., 1996).

All together, these data support the possible transport of our peptides via paracellular route. Notheworthy, the passive paracellular transport via tight junctions has been recognized for the absorption of water-soluble low molecular weight and short-chain peptides positively charged due to the average negative charge of tight junctions (Salamat-Miller & Johnston, 2005). Finally, the docking study on rubiscolin-6 and its *C*-terminal amide into DOR gave an insight on their binding mode and justifies the low potency and efficacy *in vitro*, comparing to the DOR crystallographic ligand TIPP-$NH_2$. These results are in line with the information previously obtained with CoMFA and CoMSIA models applied to rubiscolin-6 analogues (Caballero, Saavedra, Fernandez, & Gonzalez-Nilo, 2007), and represent the first temptative to expand our knowledge on the mechanism of action of these natural compounds mediated by DOR contribution.

In conclusion, we found that rubiscolin-6 *C*-terminal amide is able to exert antinociceptive effect after i.c.v. and s.c. administrations in the formalin test, at 100 μmol to stimulate opioid receptors in calcium mobilization assay. This let us suppose an activity at the central level and periphery (Cassell et al., 2019) by δ-opioid receptor modulation in light of previous studies, our docking prediction and a good pharmacological profile in terms of safety and peripheral use due to a low intestinal absorption. The potential applications of this novel peptide derived from plant involve its use as food supplement, various biotechnological products and processes.

## 5. Ethics statement

The research protocol for in vivo tests was approved by the Service for Biotechnology and Animal Welfare of the Istituto Superiore di

Sanità and authorized by the Italian Ministry of Health, according to Legislative Decree 26/14, which implemented the European Directive 2010/63/UE on the protection of laboratory animals in Italy. Animal welfare was routinely checked by veterinarians from the Service for Biotechnology and Animal Welfare.

## CRediT authorship contribution statement

**Azzurra Stefanucci:** Conceptualization, Writing - review & editing. **Marilisa Pia Dimmito:** Investigation. **Giancarlo Tenore:** Formal analysis. **Stefano Pieretti:** Data curation, Validation. **Paola Minosi:** Data curation, Validation. **Gokhan Zengin:** Data curation. **Chiara Sturaro:** Investigation. **Girolamo Calò:** Investigation. **Ettore Novellino:** Formal analysis. **Angelo Cichelli:** Conceptualization, Writing - review & editing. **Adriano Mollica:** Supervision, Software, Resources.

## Declaration of Competing Interest

The authors declare that they have no known competing financial interests or personal relationships that could have appeared to influence the work reported in this paper.

## Appendix A. Supplementary material

Supplementary data to this article can be found online at https://doi.org/10.1016/j.jff.2020.104154.

## References


Arısoy, S., & Üstün-Aytekin, O. (2018). Hydrolysis of food-derived opioids by dipeptidyl peptidase IV from Lactococcus lactis spp. Lactis. *Food Research International, 11*, 574–581.

Bigliardi-Qi, M., Gaveriaux-Ruff, C., Zhou, H., Hell, C., Bady, P., Rufli, T., ... Bigliardi, P. (2006). Deletion of delta-opioid receptor in mice alters skin differentiation and delays wound healing. *Differentiation, 74*, 174–185.

Brandsch, M., Knütter, I., & Bosse-Doenecke, E. (2008). Pharmaceutical and pharmacological importance of peptide transporters. *Journal of Pharmacy and Pharmacology, 60*, 543–585.

Caballero, J., Saavedra, M., Fernandez, M., & Gonzalez-Nilo, F. D. (2007). Quantitative structure-activity relationship of rubiscolin analogues as delta opioid peptides using comparative molecular field analysis (CoMFA) and comparative molecular similarity indices analysis (CoMSIA). *Journal of Agricultural Food Chemistry, 55*, 8101–8104.

Camarda, V., Fischetti, C., Anzellotti, N., Molinari, P., Ambrosio, C., Kostenis, E., ... Calo, G. (2009). Pharmacological profile of NOP receptors coupled with calcium signaling via the chimeric protein Gαqi5. *Naunyn Schmiedebergs Archives of Pharmacology, 379*, 599–607.

Cassell, R. J., Mores, K. L., Zerfas, Mahmoud, A. H., Lill, M. A., Trader, D. J., & van Rijn, R. M. (2019). Rubiscolins are naturally occurring G protein-biased delta opioid receptor peptides. *European Neuropsychopharmacology, 29*, 450–456.

Dimmito, M. P., Stefanucci, A., Pieretti, S., Minosi, P., Dvorácskó, S., Tömböly, C., ... Mollica, A. (2019). Discovery of orexant and anorexant agents with indazole scaffold endowed with peripheral antiedema activity. *Biomolecules, 9*, E492. https://doi.org/10.3390/biom9090492.

Dvoracsko, S., Stefanucci, A., Novellino, E., & Mollica, A. (2017). The design of multi-target ligands for chronic and neuropathic pain. *Future Medicinal Chemistry, 7*, 2469–2483.

Furkert, J., Klug, U., Slominski, A., Eichmuller, S., Mehlis, B., Kertscher, U., & Paus, R. (1997). Identification and measurement of b-endorphin levels in the skin during induced hair growth in mice. *Biochimica Biophysica Acta, 1336*, 315–322.

Grochowski, D. M., Uysal, S., Aktumsek, A., Granica, S., Zengin, G., Ceylan, R., & Tomczyk, M. (2017). In vitro enzyme inhibitory properties, antioxidant activities, and phytochemical profile of Potentilla thuringiaca. *Phytochemistry Letters, 20*, 365–372.

Hirata, H., Sonoda, S., Agui, S., Yoshida, M., Ohinata, K., & Yoshikawa, M. (2007). Rubiscolin-6, a δ opioid peptide derived from spinach Rubisco, has anxiolytic effect via activating σ1 and dopamine D1 receptors. *Peptides, 28*, 1998–2003.

Kaneko, K., Iwasaki, M., Yoshikawa, M., & Ohinata, K. (2010). Orally administered soymorphins, soy-derived opioid peptides, suppress feeding and intestinal transit via gut1-receptor coupled to 5-HT1A, D2, and GABAB systems. *American Journal of Physiology-Gastrointestinal and Liver Physiology, 299*, 799–805.

Kaneko, K., Lazarus, M., Miyamoto, C., Oishi, Y., Nagata, N., Yang, S., ... Ohinata, K. (2012). Orally administered rubiscolin-6, a δ opioid peptide derived from Rubisco, stimulates food intake via leptomeningeal lipocallin-type prostaglandin D synthase in mice. *Molecular Nutrition and Food Research, 56*, 1315–1323.

Kaserer, T., Lantero, A., Schmidhammer, H., Spetea, M., & Schuster, D. U. (2016). Opioid receptor: Novel antagonists and structural modeling. *Scientific Reports, 6*, 1–15.

Kauser, S., Schallreuter, K. U., Thody, A. J., Gummer, C., & Tobin, D. J. (2003). Regulation of human epidermal melanocyte biology by b-endorphin. *Journal of Investigational Dermatology, 120*, 1073–1080.

Kim, D.-O., Lee, K. W., Lee, H. J., & Lee, C. Y. (2002). Vitamin C equivalent antioxidant capacity (VCEAC) of phenolic phytochemicals. *Journal of Agricultural food Chemistry, 50*, 3713–3717.

Knipp, G. T., Velde, D. G. V., Siahaan, T. J., & Borchardt, R. T. (1997). The effect of beta-turn structure on the passive diffusion of peptides across Caco-2 cell monolayers. *Pharmaceutical Research, 14*, 1332–1340.

Lambert, D.G., Rainbow, R.D. (eds.), (2013). Calcium Signaling Protocols, Methods in Molecular Biology, vol. 937. Springer Science, Business Media, LLC. DOI 10.1007/978-1-62703-086-118.

Luisi, G., Stefanucci, A., Zengin, G., Dimmito, M. P., & Mollica, A. (2018). Anti-oxidant and tyrosinase inhibitory in vitro activity of amino acids and small peptides: new hints for the multifaceted treatment of neurologic and metabolic disfunctions. *Antioxidants, 8*, pii: E7. https://doi.org/10.3390/antiox8010007.

Mareček, V., Mikyška, A., Hampel, D., Čejka, P., Neuwirthová, J., Malachová, A., & Cerkal, R. (2017). ABTS and DPPH methods as a tool for studying antioxidant capacity of spring barley and malt. *Journal of Cereal Science, 73*, 40–45.

Miyazaki, Y., Kaneko, K., Iguchi, S., Mizushige, T., Kanamoto, R., Yoshikawa, M., ... Ohinata, K. (2014). Orally administered δ opioid agonist peptide rubiscolin-6 stimulates food intake in aged mice with ghrelin resistance. *Molecular Nutrition and Food Research, 58*, 2046–2052.

Mollica, A., Costante, R., Stefanucci, A., Pinnen, F., Lucente, G., Fidanza, S., & Pieretti, S. (2013). Antinociceptive profile of potent opioid peptide AM94, a fluorinated analogue of biphalin with non-hydrazine linker. *Journal of Peptide Science, 19*, 233–239.

Mollica, A., Pinnen, F., Feliciani, F., Stefanucci, A., Lucente, G., Davis, P., ... Hruby, V. J. (2011). New potent biphalin analogues containing p-fluoro-L-phenylalanine at the 4,4' positions and non-hydrazine linkers. *Amino Acids, 40*, 1503–1511.

Nwachukwu, I. D., & Aluko, R. E. (2019). Structural and functional properties of food protein-derived antioxidant peptides. *Journal of Food Biochemistry, 43*, Article e12761. https://doi.org/10.1111/jfbc.12761.

Ohinata, K., Agui, S., & Yoshikawa, M. (2007). Soymorphins, novel mu opioid peptides derived from soy beta-conglycinin beta-subunit, have anxiolytic activities. *Bioscience, Biotechnology and Biochemistry, 71*, 2618–2621.

Okumu, F. W., Pauletti, G. M., Vander Velde, D. G., Siahaan, T. J., & Borchardt, R. T. (1997). Effect of restricted conformational flexibility on the permeation of model hexapeptides across Caco-2 cell monolayers. *Pharmaceutical Research, 14*, 164–175.

Pauletti, G. M., Gangwar, S., Okumu, F. W., Siahaan, T. J., Stella, V. J., & Borchardt, R. T. (1996). Esterase-sensitive cyclic prodrugs of peptides: Evaluation of an acyloxyalkoxy promoiety in a model hexapeptide. *Pharmaceutical Research, 13*, 1615–1623.

Perlikowska, R., & Janecka, A. (2018). Rubiscolins-highly potent peptides derived from plant proteins. *Mini Reviews in Medicinal Chemistry, 18*, 104–112.

Piekielna-Ciesielska, J., Mollica, A., Pieretti, S., Fichna, J., Szymaszkiewicz, A., Zielińska, M., ... Janecka, A. (2018). Antinociceptive potency of a fluorinated cyclopeptide Dmt-c[D-Lys-Phe-p-CF 3-Phe-Asp]NH2. *Journal of Enzyme Inhibition and Medicinal Chemistry, 33*, 560–566.

Pillaiyar, T., Manickam, M., & Namasivayam, V. (2017). Skin whitening agents: Medicinal chemistry perspective of tyrosinase inhibitors. *Journal of Enzyme Inhibition and Medicinal Chemistry, 32*, 403–425.

Poli, G., Dimmito, M. P., Mollica, A., Zengin, G., Benyhe, S., Zador, F., & Stefanucci, A. (2019). Discovery of novel μ-opioid receptor inverse agonist from a combinatorial library of tetrapeptides through structure-based virtual screening. *Molecules, 24*, 3872. https://doi.org/10.3390/molecules24213872.

Raiola, A., Meca, G., Mañes, J., & Ritieni, A. (2012). Bioaccessibility of deoxynivalenol and its natural co-occurrence with ochratoxin A and aflatoxin B1 in Italian commercial pasta. *Food and Chemical Toxicology, 50*, 280–287.

Regazzo, D., Mollé, D., Gabai, G., Tomí, D., Dupont, D., Leonil, J., & Boutrou, R. (2010). The (193–209) 17-residues peptide of bovine β-casein is transported through Caco-2 monolayer. *Molecular Nutrition and Food Research, 54*, 1428–1435.

Salamat-Miller, N., & Johnston, T. P. (2005). Current strategies used to enhance the paracellular transport of therapeutic polypeptides across the intestinal epithelium. *International Journal of Pharmaceutics, 294*, 201–216.

Satake, M., Enjoh, M., Nakamura, Y., Taka, T., Kawamura, Y., Arai, S., & Shimizu, M. (2002). Transepithelial transport of the bioactive tripeptide, Val-Pro-Pro, in human intestinal Caco-2 cell monolayers. *Bioscience, Biotechnology, and Biochemistry, 66*, 378–384.

Schmelz, M., & Paus, R. (2007). Opioids and the skin: "Itchy" perspectives beyond analgesia and abuse. *Journal of Investigational Dermatology, 127* 1287–1287.

Schrödinger Release 2016-4: LigPrep, Schrödinger, LLC, New York, NY (2016).

Schurink, M., van Berkel, J. W., Wichers, H. J., & Boeriu, C. G. (2007). Novel peptides with tyrosinase inhibitory activity. *Peptides, 28*, 485–495.

Stefanucci, A., Dimmito, M. P., Macedonio, G., Ciarlo, L., Pieretti, S., Novellino, E., ... Mollica, A. (2020). Potent, efficacious, and stable cyclic opioid peptides with long lasting antinociceptive effect after peripheral administration. *Journal of Medicinal Chemestry, 63*, 2673–2687.

Stefanucci, A., Lei, W., Pieretti, S., Novellino, E., Dimmito, M. P., Marzoli, F., ... Mollica, A. (2019). On resin click-chemistry-mediated synthesis of novel enkephalin analogues with potent anti-nociceptive activity. *Scientific Reports, 9*, 5771. https://doi.org/10.1038/s41598-019-42289-5.

Stefanucci, A., Luisi, G., Zengin, G., Macedonio, G., Dimmito, M. P., Novellino, E., & Mollica, A. (2019). Discovery of arginine-containing tripeptides as a new class of pancreatic lipase inhibitors. *Future Medicinal Chemistry, 11*, 5–19.

Stefanucci, A., Mollica, A., Macedonio, G., Zengin, G., Ahmed, A. A., & Novellino, E. (2018). Exogenous opioid peptides derived from food proteins and their possible uses

as dietary supplements: A critical review. *Food Review International, 34*, 8755–9129.
Tenore, G. C., Campiglia, P., Giannetti, D., & Novellino, E. (2015). Simulated gastro-intestinal digestion, intestinal permeation and plasma protein interaction of white, green, and black tea polyphenols. *Food Chemistry, 15*, 320–326.
Tobin, D. J., & Kauser, S. (2005). Beta-endorphin: The forgotten hair follicle melano-tropin. *Journal of Investigative Dermatology Symposium Proceedings, 10*, 212–216.
Torino, D., Mollica, A., Pinnen, F., Feliciani, F., Lucente, G., Fabrizi, G., ... Hruby, V. J. (2010). Synthesis and evaluation of new endomorphin-2 analogues containing (Z)-α, β-didehydrophenylalanine (δZPhe) residues. *Journal of Medicinal Chemistry, 53*, 4550.
Yang, S., Sonoda, S., Chen, L., & Yoshikawa, M. (2003). Structure-activity relationship of rubiscolins as delta opioid peptides. *Peptides, 24*, 503–508.
Yang, S., Yunden, J., Sonoda, S., Doyama, N., Lipkowski, A. W., Kawamura, Y., & Yoshikawa, M. (2001). Rubiscolin, a delta selective opioid peptide derived from plant Rubisco. *FEBS Letters, 509*, 213–217.
Yoshikawa, M. (2015). Bioactive peptides derived from natural proteins with respect to diversity of their receptors and physiological effects. *Peptides, 72*, 208–225.
Zengin, G., Stefanucci, A., Rodrigues, M. J., Mollica, A., Custodio, L., Zakariyyah, M. A., & Mahomoodally, M. F. (2019). Scrophularia lucida L. as a valuable source of bioactive compounds for pharmaceutical applications: In vitro antioxidant, anti-inflammatory, enzyme inhibitory properties, in silico studies, and HPLC profiles. *Journal of Pharmaceutical and Biomedical Analysis, 162*, 225–233.
Zioudrou, C., Streaty, R. A., & Klee, W. A. (1979). Opioid peptides derived from food proteins. The exorphins. *Journal of Biological Chemistry, 254*, 2446–2449.
Zolghadri, S., Bahrami, A., Hassan, K., Munoz-Munoz, M. T., Garcia-Molina, J., Garcia-Canovas, F., & Saboury, A. (2019). A comprehensive review on tyrosinase inhibitors. *Journal of Enzyme Inhibition and Medicinal Chemistry, 34*, 279–309.